U-series and radiocarbon cross dating of speleothems from Nerja Cave (Spain): Evidence of open system behavior. Implication for the Spanish rock art chronology

E. Pons-Branchu, J. Barbarand, I. Caffy, A. Dapoigny, L. Drugat, J.P. Dumoulin, M.A. Medina Alcaide, J. Nouet, J.L. Sanchidrián Torti, N. Tisnérat-Laborde, et al.

U-series and radiocarbon cross dating of speleothems from Nerja Cave (Spain): evidence of open system behavior. Implication for the Spanish rock Art chronology.

Pons-Branchu E.[1], Barbarand J.[2], Caffy I[3], Dapoigny A.[1], Drugat L. [1], Dumoulin J.P. [3], Medina Alcaide M.A. [4,5], Nouet J. [2], Sanchidrián Torti J.L. [5], Tisnérat-Laborde N.[1], Jiménez de Cisneros C.[6], Valladas H.[1]

1. LSCE : Laboratoire des Sciences du Climat et de l'Environnement, LSCE/IPSL, CEA-CNRS-UVSQ, Université Paris-Saclay, F-91191 Gif-sur-Yvette, France.
2. GEOPS : Laboratoire GEOPS, Université. Paris Saclay – UMR 8148 CNRS – Université Paris Saclay, 91405 Orsay Cedex, France.
3. Laboratoire de Mesure du Carbone 14 (LMC14), LSCE/IPSL, CEA-CNRS-UVSQ, Université Paris-Saclay, 91191, Gif-sur-Yvette, France
4. PACEA UMR 5199, UNIVERSITÉ DE BORDEAUX, Bâtiment B2, Allée Geoffroy Saint-Hilaire CS 50023, 33615 PESSAC Cedex.
5. University of Cordoba UCO, Department of History (HUM-781)Cardenal Salazar s/n, 14071 Cordoba, Spain
6. Instituto Andaluz de Ciencias de la Tierra (CSIC-UGR), Avda. de las Palmeras 4, Armilla, 18100, Granada, Spain

Abstract

Two stalagmites from Nerja cave (Andalusia, Spain) were studied. The cave is well known because of its long human occupation from the Upper Palaeolithic to the Chalcolithic and its abundant parietal prehistoric Art. The aims of this study were twofold: i) to compare uranium/thorium ($^{230}Th/^{234}U$) and Carbon-14 (^{14}C) ages obtained all along the growth axis of the stalagmites in order to understand the consequences of diagenetic processes on the validity of radiometric ages; ii) as one of the stalagmites contains black layers, attributed to combustion soot, to establish when these intense hearths were used and by which culture.

$^{230}Th/^{234}U$ and ^{14}C ages were coupled with mineralogical studies using FTIR (Fourier-transform infrared spectroscopy) and thin section observations. The first stalagmite (GN16-9b) displays $^{230}Th/^{234}U$ ages in stratigraphic order, and compatible with ^{14}C ages corrected for a few percent of dead carbon. Homogeneous composition of aragonitic crystals characterized by their needle-like texture is observed throughout this speleothem. For the

second stalagmite (GN16-7), in contrast, ^{230}Th/^{234}U ages display large significant inversions and discordant results on the upper part and at the base of the stalagmite, suggesting a possible open system behavior for this chronometer. Interestingly, ^{14}C ages are in stratigraphic order all along the stalagmite and are compatible with ^{230}Th/^{234}U ages only in its central part. Mineralogical studies display evidence of aragonite to calcite transformation at the top and a complex mineralogical assemblage with interlayered silicates (possibly clays) and calcitic mineralogy for the base of GN16-7. In these parts, discordant ^{230}Th/^{234}U ages were measured. In the middle part of the stalagmite, however, where the fibrous aragonite is well preserved, the ^{14}C and ^{230}Th/^{234}U ages agree. Our data suggest that in the case of aragonite to calcite transformation as shown here, ^{230}Th/^{234}U ages are biased, but ^{14}C ages seem to remain accurate, as already observed in aragonitic marine bio minerals. ^{14}C ages obtained are used for the chronology of the soot layer, determined here between 7,900 and 5,500 years cal BP, coherent with previous analysis of charcoals in the same sector of the cave. This study highlights the importance of working with at least two chronometers when stratigraphic age verification is not possible, as is the case of some parietal CaCO$_3$ thin layers used for rock art dating. Recent ^{230}Th/^{234}U ages published for carbonate deposits on Spanish parietal Art are discussed in light of this demonstration.

1. Introduction

Diagenetic processes are an important issue when dealing with the chronology of secondary carbonate deposits found in caves or marine environments, for both archaeological and paleo-environmental studies. These processes have been extensively studied in corals, for which clear criteria of age validity are defined, requiring a pure aragonite mineralogy and uranium (U) isotopic composition compatible with that of the oceans at the time of mineral formation (e.g. Thompson et al., 2013; Andersen et al., 2010). For speleothems, such "universal" criteria do not exist because the U isotopic composition of continental waters is highly variable, and the initial mineralogy can be composed of either aragonite or calcite (two polymorphs of CaCO$_3$), or a mixture of the two. Aragonite to calcite transformation is one of the most extensively documented diagenetic processes for speleothems (Folk and Assereto, 1976), with the identification of uranium-thorium (or U/Th or ^{230}Th/^{234}U) age inversions at odds with the stratigraphic position (Railsback et al., 2002; Ortega et al., 2005;

Perrin et al., 2014; Scholz et al., 2014). Secondary fluids are responsible for this recrystallization and therefore the definition of an open or semi-closed system is critical to assess age validity (Domínguez-Villar et al., 2017). Other phenomena of post-depositional alteration may be highlighted where no macroscopic change is visible but micro-voids are observed (Bajo et al., 2016).

These dating difficulties due to diagenetic processes are particularly problematic for carbonate layers deposited on cave walls where they are often too thin to allow demonstrating stratigraphic coherence of the datations. These deposits are however studied with increasing interest. The ^{230}Th/^{234}U chronology of $CaCO_3$ layers covering or underlying rock art has been used for several decades in order to determine a minimum or maximum age of the representations (Bischoff et al., 2003), with in some cases unexpectedly old ages for Spanish rock art (Pike et al., 2012; Hoffman et al., 2018). Their validity has, however, been questioned based on archaeological (Aubert et al., 2018; Clottes, 2012; White et al., 2020) and geochemical evidence (Pons-Branchu et al., 2014a; Pearce and Bonneau, 2018; Slimak et al., 2018; Pons-Branchu et al., 2020), although see responses to criticisms in (Hoffmann et al. 2018, 2019, 2020). In order to verify the validity of the ages determined, some authors tried whenever possible to have ages along a stratigraphy (e.g. Hoffmann et al., 2018, Aubert et al., 2019; Wu et al., 2022) or to perform cross-dating between U-series and ^{14}C chronometers (Fontugne et al., 2013; Corchón Rodríguez et al., 2015; Shao et al., 2021; Shao et al., 2017; Valladas et al., 2017).

This paper is based on the study of two speleothems that grew in two distinct zones of the Nerja cave. In these zones, thin $CaCO_3$ layers covering or overlying rock art were previously studied using ^{14}C dating (Sanchidrian et al., 2017), or ^{230}Th/^{234}U dating (Pons-Branchu et al., 2020) or both methods (Valladas et al., 2017). For some samples, there was evidence of age validity but for others, an open system behavior was suspected. In this paper, by studying two stalagmites of the same cave, we will discuss possible mechanisms of open system behavior in relation with the influence of the geological and environmental context of the cave itself; other caves located in similar geological environments could be affected by the same phenomena.

2. Site and samples

Nerja cave (Andalusia, southern Spain, see location in Fig. 1), is a large (4843 m in length) cavity located on the border of the Sierra Almijara within the Betic Cordillera. It is developed on triassic carbonate marbles of a dolomitic nature (Sanz de Galdeano, 1990). Two fossil gallery levels – labelled lower and upper galleries - host large and diversified speleothem formations, some of them of very large dimensions, among which columns measuring several meters in diameter. Nerja cave hosts important parietal art, with figurative representations (horses, ibex, deer…) and non-figurative signs and marks (Sanchidrián, 1994; Sanchidrián et al., 2001, 2017). Few representations were drawn with charcoal, and the majority of them, made with red pigments, cannot be datable by ^{14}C method.

Previous studies on speleothems at Nerja cave were conducted on aragonitic stalagmite and stalactite whose growth periods were dated between respectively 90 and 70 ka (Jiménez de Cisneros and Caballero 2011), and 190 to 160 ka (Jiménez de Cisneros et al., 2003).

In the present study, two speleothems were sampled and studied (Fig. 1c). Their longitudinal sections show well developed macroscopic to microscopic laminations (Fig.1).

These two speleothems GN16-7 and GN16-9b originated from areas where thin carbonate layers deposited on the decorated walls were previously dated by U/Th or ^{14}C or by both methods (Sanchidrián et al., 2017; Valladas et al. 2017; Pons-Branchu et al., 2020).

Stalagmite GN16-7 was found broken on the upper galleries, at the end of the *Pisciform Chamber*. The stalagmite is 12 cm high, well laminated, and does not present any perturbations visible to the naked eye such as dissolution processes, except at the base and on an infra centimetric layer in the middle of the sample, just before a thin dark layer.

Stalagmite GN 16-9b (Fig. 1c) was found lying on a sandy level of the lower gallery, in the sector of the "red child grave", in the *Cataclysm Hall*. The stalagmite is 5 cm high, with a section showing "diffuse" lamination, and fibers visible to the naked eye. It grew at the bottom on detrital carbonate clasts.

3. Materials and Methods

Each stalagmite was cut in half along the growth axis using a diamond saw. Polished thin sections were prepared from the different parts of the stalagmites and for petrographic and mineralogical observation. Samples of $CaCO_3$ of about 100 mg of millimetric fragments were extracted all along the growth axis and split into two portions: 10 mg was taken for ^{14}C analysis and the remaining sample, between 40 and 90 mg, was kept for U-series analysis. Ten levels were sampled for GN16-7, and six for GN16-9b.

3.1.   Petrography and mineralogy

Samples were observed on 30 μm thin sections with an optical microscope (Leica) at a magnification between x25 and x100 in plane polarized light (PPL) and in cross-polarized light (CPL). FT-IR mappings were performed on a Spotlight 400 (Perkin-Elmer) imager at the Paris Saclay Geosciences laboratory (GEOPS, Paris Saclay University) on the same rock pieces used for thin section preparation. The imager is equipped with an MCT (mercury cadmium telluric) array detector and mappings were obtained on polished surfaces in reflection and/or ATR (Attenuated Total Reflectance) imaging modes. Measurements were performed using a 4000-690 cm^{-1} spectral range with a 4 cm^{-1} spectral resolution and a 2 cm^{-1} interval. Each pixel was scanned twice, with a point resolution of 6.25x6.25 μm by pixel. FT-IR can be used to identify carbonate minerals (Huang and Kerr, 1960), using the "in-plane" (ν4) and "out-of-plane" (ν2) bending modes of their CO_3^{2-} vibration. Aragonite is characterized by a doublet ν4 vibration at 700 and 712 cm^{-1} and a ν2 band at ~855 cm^{-1}. The calcite-magnesite solid-solution is characterized by single ν4 and ν2 vibrations, which display a regular shift depending on the amount of Mg^{2+} substituted to Ca^{2+} in its lattice site: ν4 is at 712, 728 and 748 cm^{-1} and ν2 at ~875, ~881 and ~887 cm^{-1}, respectively for pure calcite, dolomite and magnesite (Andersen and Brečević, 1991). The position of the carbonate absorption band ν2 and its width (sigma x2) can serve as proxies for variations in the crystal parameters of these mineral phases.

3.2.   Radiocarbon analysis

The fifteen $CaCO_3$ samples were hydrolyzed with H_3PO_4 to obtain CO_2 and converted to graphite as described by Tisnérat-Laborde et al. (2001) and Dumoulin et al. (2017). They were measured at the Artemis AMS-French National facility (CEA Saclay, LMC14; Moreau et al., 2020). The ^{14}C measurements were corrected to the isotopic fractionation according to the $\delta^{13}C$ values measured on the AMS, following international recommendations (Mook and van der Plicht, 1999).

^{14}C results were calibrated using OxCal 4.4 (Ramsey C.B. 2006) and the Intcal20 data (Reimer et al. 2020) i) with no correction for dead carbon proportion (DCP), and ii) with a 10% DCP correction, following Sanchidrian et al., (2017).

3.3. Uranium-series analysis

Samples were dissolved in Teflon™ PFA beakers where a known amount of a ^{229}Th-^{236}U spike calibrated against HU-1 Uraninite had been previously added. After coprecipitation with FeOH, uranium (U) and thorium (Th) fractions were separated from the matrix and purified using U-TEVA® resin in nitric media following a protocol modified from Pons-Branchu et al. (2005) and detailed in Pons-Branchu et al. (2014b). U and Th fractions were measured using a multi-collector inductively coupled plasma mass spectrometer (MC-ICP-MS) Thermo Scientific™ Neptune Plus fitted with a jet pump interface and an Aridus™ II desolvating system. ^{238}U, ^{235}U, ^{236}U and ^{229}Th were measured on Faraday cups, ^{234}U and ^{230}Th on the ion counter. 10^{12} Ω amplifiers were used for isotopes ^{229}Th, ^{236}U, ^{232}Th and 10^{11} Ω amplifiers for ^{235}U and ^{238}U isotopes. Ages were corrected for detrital fraction, assuming a ^{230}Th/^{232}Th activity ratio of 1.5 ± 50% (Hellstrom, 2006).

3.4. Black level analysis

Transmission electron microscopy – Energy Dispersive X-ray spectroscopy (TEM-EDX) allows the characterization of the anatomical structure at nanometric scale of solid samples and the production of analytical maps. This tool was previously used to characterize soot layers of speleothems from the Dominica cave in Slovakia (Pawlyta and Hercman, 2016).

The sample, a powder extracted by scraping the black level of the stalagmite with a scalpel, was prepared following Pawlyta and Hercman (2016): after acid dissolution with 1M HCl, the sample was rinsed with distilled water, and finally filtrated to obtain nano-sized particles to be analysed using TEM-EDX. TEM-EDX analyses were performed at the University of Malaga, using a FEI Talos F200X apparatus.

4. Results

4.1. *Petrography and mineralogy*

Sample GN16-9b is composed of only slightly marked growth bands individualized by slight variations in color. The whole sample is criss-crossed by millimetric fibers. Only the outer band is a little different with a more matt appearance and the absence of fibers. Optical microscopy confirmed the homogeneous texture of the elongated millimetric crystals with an axial or fan-shaped growth (Fig. 2a). Most of the crystals are not coalescing which produces a large porosity in the sample. The outer band is built of smaller fibers and separated from the main part by a thin dark layer (Fig. 2b). The infra-red image shows the homogeneity of the sample with the exclusive presence of aragonite (v2 band < 860 cm^{-1}) in the main part but also in the outer layer with a relatively large standard deviation (~15-17 cm^{-1}) of the v2 band, indicating poor crystallinity (Fig S.M. 1).

Macroscopically, the GN16-07 concretion is made up of three parts: a base with irregular yellow growth bands and a grey core, an intermediate part with continuous growth and some levels of high porosity, and a final part of homogeneous white crystals. Optical microscopy identified a dominant fibrous texture in plane polarized light (PPL) and in cross-polarized light (CPL) (Fig. 3 a: example of the second part of the core) corresponding to the central part of the concretion. The lower part shows continuous growth beds, sometimes dark, with mosaic crystals visible in cross-polarized light (Fig. 3 b: example of mosaic crystals in CPL) and crystals with fibrous texture. The top part shows bands of continuous growth with a fibrous texture (Photo C: PPL and CPL photo of the top section, Fig 3c).

The mineralogy defined from the infra-red imaging showed three phases: a major aragonitic phase, a minor calcitic phase except in the top part and a silicate phase observed only in the basal part (Fig. 4 and Fig S.M. 2: FT-IR image of the concretion). The basal calcite phase is well crystallized (narrow peaks ~14 cm^{-1}) and in the position of a standard calcite. In the intermediate part, the aragonitic phase evolves, with a very slight decrease in crystallinity (sigma from ~11 to ~13 cm^{-1}) and in the position of the $\nu 2$ band (from 859 to 854 cm^{-1}), which can be correlated with a variation in Sr content. Two small bands of a very different aragonite (sigma ~11 cm-1 and position at 849 cm^{-1}) are observed at the end of this growth episode, followed by a poorly crystallized band (sigma ~16 cm^{-1}). The top calcitic phase is less well crystallized than the basal phase (sigma ~17 cm^{-1}), and appears to be composed of two phases, with an increase in the position of the $\nu 2$ band (from 866 to 872 cm^{-1}), which may correlate with an increase in Mg content substituted for Ca. For the base, the silicates could correspond to detrital clays contemporary with the early phases of concretion growth (Fig. 4).

4.2. Dating results

Eight ^{230}Th/^{234}U dating results were obtained for the stalagmite GN16-7, and six for GN16-9b. The two stalagmites display variable U content, between 1.50 ± 0.01 and 3.32 ± 0.03 ppm for GN16-9b and between 0.76 ± 0.01 and 8.40 ± 0.03 ppm for GN16-7. U isotopic composition is close to equilibrium, with δ^{234}U between 24.8 ± 1.0 and 31.0 ± 1.3 ‰ for GN16-9b and between 1.8 ± 1.0 and 13.5 ± 1.7 ‰ for GN16-7. All the studied sub samples display low detrital Th, with ^{232}Th lower than 4 ppt and ^{230}Th/^{232}Th activity ratios higher than 123. ^{230}Th/^{234}U ages agree with their stratigraphic order (from 2150 ± 24 to 4314 ± 83 years cor BP) for stalagmite GN16-9b but display marked age inversions for stalagmite GN16-7 (age range between 7561 ± 165 years and 17784 ± 261 years cor BP), with much older ages in the upper part and at the base of the speleothem. On the contrary, ^{14}C ages (assuming 0 or 10% of DCP) are coherent with stratigraphic order for the two stalagmites.

Interestingly, for stalagmite GN16-9b, ^{230}Th/^{234}U ages fall in the same range as ^{14}C ages with 0 and 10% DCP correction (Fig. 5). For stalagmite GN16-7, only the aragonitic central part of the stalagmite gives agreement between the two methods (Fig. 4). Three little exceptions for ^{230}Th/^{234}U and ^{14}C ages agreement within the aragonitic parts of the stalagmites were found.

The first one (ca 200 years), for GN19b at 36 cm, could be explained by a higher value of the isotopic composition of the detrital phase (a $^{230}Th/^{232}Th$ activity ratio of the detrital phase around 7 makes the ages compatible) or a non-homogeneous sample between ^{14}C and $^{230}Th/^{234}U$ fractions. A high value of the isotopic composition of the detrital phase is not unrealistic for this cave, because in another study of the Nerja cave (Valladas et al., 2017), we analyzed present day $CaCO_3$ samples and found a high $^{230}Th/^{232}Th$ activity ratio (5.2 ± 0.3). This value can be slightly variable at the scale of the cave. For the two other levels (GN16-7 at 46 and 29.5 mm), the age difference, respectively of 300 and 1000 years is too important to be explained by a high isotopic composition of the detrital value. The two hypotheses are 1) some minor diagenetic alteration, but below the detection limits of our methodology ; 2) a difference due to the sampling position between $^{230}Th/^{234}U$ and ^{14}C fractions. Indeed, in order to avoid contamination by modern carbon during the preparation, we use small pieces of samples extracted from the growth axis of the speleothem, and not homogenized powder resulting from the grinding of the pieces used for both analyses.

4.3.   Black level analysis

TEM-EDX observation revealed spherical particles of soot aggregates (Fig. 6) similar to those found at the Dominica cave (Pawlyta and Hercman, 2016). Similar particles were observed at Nerja cave inside a Palaeolithic fixed lamp from the upper galleries, close to the studied stalagmite (Medina-Alcaide 2019), but also inside a speleothem fragment sited in the Cataclysm Hall (del Rosal, 2016). Our analyses thus confirm that the black levels observed in the GN16-7 stalagmite resulted from particulate emissions from the combustion of wood, with visible concentric nanoparticles (Kocbach et al. 2006).

5. Discussion

5.1.   Age bias: identification and causes

^{14}C ages (assuming DCP between 0 and 10%) and $^{230}Th/^{234}U$ ages generally agree for the GN16-9b stalagmite, made of pure aragonite, and for the aragonitic part of GN16-7. For this

speleothem, ^{14}C ages remain in stratigraphic order for calcitic sections (top and base of the stalagmite), while this is not the case for [230]Th/[234]U ages, which display marked age inversions (Fig. 4 and 5).

The alternation of aragonite and calcite in speleothem GN16-7 is not an unequivocal marker of diagenesis as both the aragonite and calcite may be primary, alternating in the same speleothem due to changes in environmental parameters (Railsback et al. 1994; McMillan et al. 2005, Wassenburg et al., 2012). The criteria that we used in this study to detect recrystallization was the difference between the texture and the mineralogy. In the outer part of sample GN16-07, a calcite phase characterized by FT-IR is made of elongated columnar crystals which are typical of aragonitic mineralogy. Age inversion and disagreement between the two chronometers occurred only in these calcitic parts. In order to test the hypothesis of a [230]Th/[234]U bias due to aragonite to calcite transformation, we present age difference ([230]Th/[234]U cor age minus ^{14}C age cal BP with 0% DCP assumed to be real age) against U content (Fig. 7). For the samples within the aragonitic part, U content is high (> 3.59 ppm), and the age difference between [230]Th/[234]U and ^{14}C ages is minimal, whereas for calcitic sections, U content is low (< 0.9 ppm at the top and 1.7 ppm for the base level) and the age difference is larger, with [230]Th/[234]U ages that are systematically too old (Fig. 7). This observation is coherent with U leaching by circulation fluids during the aragonite to calcite transformation, causing apparent aging of the sample, as already observed for speleothems from several countries such as Spain, France, Egypt, Mexico (e.g. Ortega et al., 2005; Lachniet et al., 2012; Railsback et al., 2002; Domínguez-Villar et al., 2017). This agrees with the observation of an increase in the [230]Th/[234]U ratio (and apparent age) with low U content, observed for samples from "*Panel de las focas*" from the *Pisciform Chamber* of the Nerja cave upper gallery, and the hypothesis put forward of U loss causing too old ages for part of the studied samples (Pons-Branchu et al., 2020). Interestingly, this transformation does not appear to affect ^{14}C ages, which in the present case remain coherent, unlike [230]Th/[234]U ages. This has already been observed for marine $CaCO_3$ samples (e.g. Lindauer et al., 2018). The validation of ^{14}C chronology is coherent with the fact that the aragonite to calcite transformation does not seems to affect the carbon isotopic composition as shown by the study of Zhang et al. (2014).

The present study confirms that at Nerja cave, ^{14}C ages on $CaCO_3$ samples can be used for their chronology, as underlined by Sanchidrián et al. (2017) where a $CaCO_3$/charcoal/$CaCO_3$ sequence was successfully dated by ^{14}C. In this study, we also confirm that at Nerja cave, DCP is small (between 0 and 10%) probably in relation with low dissolution of the host rock (Genty et al., 2001).

5.2.   Soot level on the GN16-7 stalagmite and past illumination at Nerja cave

^{14}C ages are reliable throughout stalagmite GN16-7, and they were used for the chronology of the soot level. Interestingly, this level corresponds to the transition between aragonite to calcite, and to a growth hiatus evidenced by ^{14}C ages. We consider that there is no link between recrystallisation and this event. Even if fire and high temperature may play a role in mineralogical transformation (Toffolo et al., 2021 and references therein), this soot level appears anterior to the deposition of the altered outer part of the stalagmite. The soot level is composed of a series of sub levels, at least 4 (see picture in Fig. 8), attesting the recurrence of fires and/or of the different visits at this place in the cave. The fire was possibly used as a light source, as demonstrated by Medina Alcaide (2019), Medina-Alcaide and Sanchidrián (2014), and Medina Alcaide et al. (2015). The depth of these soot laminae is ca 24 mm from top. For a rough estimate of their age (upper and lower limit), we use ^{14}C data with 0 % DCP for the $CaCO_3$ levels before and after this soot level (at 5,584-5,472 years cal BP and 7,866-8,010 years cal BP).

According to ^{14}C chronology, these soot levels were deposited between ca 7,900 and 5,500 years cal BP, at the transition from the Epipaleolithic period to ancient and final Neolithic occupation (Medina-Alcaide, 2019). This result fits very well with a previously dated charcoal located very close to the sampling site of this stalagmite, that yielded 7,620-7,570 years cal BP (Beta 396385) which is compatible with the proposed chronology for the black soot levels. This charcoal was found scattered with others, but without other remains of combustion (rubefaction or ashes for example), and was therefore assumed to be the remains of a wooden torch lamp.

5.3. *Importance of the aragonite to calcite transformation for the validity of Spanish rock art dating using ^{230}Th/^{234}U ages*.

At Nerja cave, biased ^{230}Th/^{234}U ages were evidenced by 1) correlation between U content and apparent ages (or ^{230}Th/^{234}U ratios) for the *Pisciform Chamber*, see Pons-Branchu et al., (2020) and 2) by cross-dating between the ^{14}C and ^{230}Th/^{234}U chronometers (Valladas et al., 2017). In the latter study, the comparison between the two methods invalidated apparent very old ^{230}Th/^{234}U ages (e.g. 60 ka cor BP), obtained for the *Fantasma Hall*, indicating that geochemical alteration had affected the sample. On the contrary, in the case of the *Cascada Balcony,* the good agreement between the ^{14}C and ^{230}Th/^{234}U analyses suggests that the sample was not subjected to post deposition alteration and that the ages are reliable (ca 25,000 years cal BP). This result indicates that this type of non-figurative red representation is older than 25,000 years cal BP and that it can be associated with the oldest attested Palaeolithic occupation of Nerja Cave. This age range of carbonated crust deposited over rock art during glacial time was recently confirmed in another decorated panel from the same part of the cave (Barbarand et al., submitted, with a calcitic crust at ca 22,000 years Cal BP).

 With the two studied stalagmites, we evidenced that the aragonite to calcite transformation caused biased ^{230}Th/^{234}U ages for the one affected, while ages remained coherent for the one not affected. The aragonite to calcite transformation is not the only mechanism responsible for potential diagenesis and biased ages for speleothems (e.g. Bajo et al., 2016, Barbarand et al. submitted), but is common in caves that contain aragonitic speleothems.

The aragonite to calcite transformation, or the presence of aragonite showing indications of alteration, is not limited to speleothems from Nerja cave for the Iberic peninsula and has been described in numerous speleothems from Spanish caves. They include : the Cave of Marvels in Aracena, Andalousia, southern Spain (Pulido-Bosch et al., 1997); Eagle cave in Avila (Domínguez-Villar et al., 2017), and Castañar cave in Extremadura (Martín-García et al., 2009; 2019), center Spain; Basajaún Etxea cave, Navarra, (Martín-García et al., 2014), and Altamira cave (Cañaveras et al., 1999, Sánchez-Moral et al., 1999), northern Spain.

In other Spanish caves, aragonite formation was identified, such as Cova da Arcoia (Galicia Province, Railsback et al., 2011), at El Soplao and Torca Ancha Caves Cantabria, (Gázquez et al., 2012, Rossi and Lozano, 2016), at Cueva Mayor, Atapuerca (Martínez-Pillado et al. 2010), at Valportero cave (Durán Valsero et al., 2000).... Until now, however, no specific study has been conducted on possible diagenetic alteration.

This abundance of aragonitic formations may be due to the presence of dolostone in a large part of karstic Spanish regions, including the Nerja cave area, but also areas that host decorated caves studied for ^{230}Th/^{234}U dating of $CaCO_3$ crusts covering rock art. This geologic formation favors high Mg/Ca ratios within cave drip waters, and thus aragonitic speleothem formation (Curl, 1962; Frisia et al., 2002; McMillan et al., 2005; Fairchild and Treble, 2009; Toffolo et al., 2021).

In this context, a deeper geochemical study (including cross dating or/and mineralogical study or/and stratigraphic studies) is needed in order to validate or reject ages obtained for the indirect dating of Spanish rock Art using $CaCO_3$ crusts, and especially when major paradigm shifts in research are being announced.

6. Conclusion

The study of two speleothems from Nerja cave, Spain, shows that alteration of the primary mineralogy may develop even if not visible macroscopically, but can be characterized by petrographical and mineralogical studies. Speleothems in aragonite preserve initial chronological information for both ^{230}Th/^{234}U and ^{14}C chronometers, but aragonite to calcite transformation induces biased ^{230}Th/^{234}U ages, and in our case study unaltered ^{14}C ages. This study echoes previous dating of $CaCO_3$ crusts covering rock art at Nerja cave, with in some cases the validation of the dating at ca 23 000 years cal BP and in other cases the invalidation of older ages, biased by U loss. ^{14}C chronology was used with a low dead carbon proportion, to determine the age of a group of layers that contain soot, between ca 5500 to ca 7900 years cal BP. These soot layers are attributed to the lighting of fires and different prehistoric visits inside the cave, on the upper galleries. This diagenetic process affecting an aragonitic speleothem at Nerja cave questions recently published Spanish rock Art indirect dating using only the ^{230}Th/^{234}U method on $CaCO_3$ thin layers. Indeed, the geological context

(presence of dolostone) is favorable to the formation of aragonite in part of these caves (Altamira cave for instance), and the aragonite to calcite transformation in speleothems has already been demonstrated in several previous studies on Spanish caves, but also in several karstic regions from other countries. Further study should be dedicated to checking for age validity, by mineralogical study and/or by cross dating.

Acknowledgements

References

Andersen, F. A. and Brecevic, L. 1991. Infrared Spectra of Amorphous and Crystalline Calcium Carbonate. Acta Chemica Scandinavica,45, 1018.

Andersen, M.B., Stirling, C.H., Zimmermann, B., Halliday, A. N. 2010. Precise determination of the open ocean 234U/238U composition. Geochem., Geophys., Geosys., 11, Q12003

Aubert, M., Brumm, A., Huntley, J., 2018. Early dates for 'Neanderthal cave art' may be wrong. *Journal of Human Evolution*, *125*, 215-217.

Aubert, M., Lebe, R., Oktaviana, A. A., Tang, M., Burhan, B., Hamrullah, Jusdi A., Hakim A.B., Zhao J.X., Geria I.M, Sulistyarto P.H., Sardi R., Brumm, A. 2019. Earliest hunting scene in prehistoric art. Nature, 576(7787), 442-445.

Bajo, P., Hellstrom J., Frisia, S., Drysdale, R., Black, J., Woodhead, J., Borsato, A., Zanchetta, G., Wallace, M.W., Regattieri, E., Haese R., 2016. "Cryptic" diagenesis and its implications for speleothem geochronologies. Quat. Sci. Reviews, 148, pp.17-28.

Barbarand, J., Pons-Branchu, E., Nouet, J., Pagel, M., Medina-Alcaide, M.A, Sanchidrián, J.L., Michelet, A., Valladas, H. (submitted). Radiometric dating of carbonated wall-crusts in the decorated Nerja cave (Spain): petrographic, mineralogical and geochemical controls.

Bischoff, J, García-Diez, M, González Morales, M.R., Sharp, W. 2003. Aplicación del método de series de Uranio al grafismo rupestre de estilo paleolítico : el caso de la cavidad de Covalanas (Ramales de la Victoria, Cantabria). Veleia 20:143–50.

Cañaveras, J. C., Hoyos, M., Sanchez-Moral, S., Sanz-Rubio, E., Bedoya, J., Soler, V., Groth, I., Scumann, P., Laiz, L., Gonzalez, I., Saiz-Jimenez, C. 1999. Microbial communities associated with hydromagnesite and needle-fiber aragonite deposits in a karstic cave (Altamira, Northern Spain). Geomicrobiology Journal, 16(1), 9-25.

Clottes, J. 2012. Datations U-Th, évolution de l'art et Néandertal. International Newsletter on Rock Art 64:1–6.

Corchón Rodríguez, S., Garate, D., Rivero, O., de la Cierva J., Valladas, H., Pons-Branchu, E**.,** Murelaga, X., Ortega, P., Vicente, F.J. 2015. U-series and 14C datings for a newly discovered decorated area in the Palaeolithic cave of La Peña de Candamo (Asturies, Northern Spain). Journal of Archaeological Science, report, 3. 371–380.

Del Rosal Padial, Y. R. 2016. Análisis, impacto y evolución de biofilms fotosintéticos en espeleotemas. El caso de la Cueva de Nerja. PhD tesis. Universidad de Malaga.

Curl, R.L. 1962. The aragonite–calcite problem**,** NSS Bull., 24–2, 57-73.

Domínguez-Villar, D., Krklec, K., Pelicon, P., Fairchild, I.J., Cheng, H., Edwards, L.R. 2017. Geochemistry of speleothems affected by aragonite to calcite recrystallization–Potential inheritance from the precursor mineral. Geochim. et Cosmochim. Acta, 200, 310-329.

Dumoulin, J.P., Comby-Zerbino, C., Delqué-Količ, E., Moreau, C., Caffy, I., Hain, S., Perron, M, Thellier, B., Setti, V., Berthier, B., Beck, L. 2017. Status report on sample preparation protocols developed at the LMC14 Laboratory, Saclay, France: from sample collection to 14C AMS measurement. Radiocarbon, 59(3), 713-726.

Durán Valsero, J.J., López Martínez, J., Dallai, L., Bruschi, G., Caballero, E., Jiménez de Cisneros, C., Julià, R. 2000. Palaeoenvironmental reconstruction based on a detailed stable isotope analysis and dating of a Holocene speleothem from Valporquero Cave, Northern Spain. Geogaceta, 27. 63-66.

Fairchild, I.J., Treble, P.C. 2009. Trace elements in speleothems as recorders of environmental change. Quat. Sci. Rev., 28(5-6), 449-468.

Frisia, S., Borsato, A., Fairchild, I.J., McDermott, F., Selmo, E.M. 2002. Aragonite-calcite relationships in speleothems (Grotte de Clamouse, France): environment, fabrics, and carbonate geochemistry. Journal of Sedimentary Research, 72(5), 687-699.

Folk, R.L., Assereto, R. 1976. Comparative fabrics of length-slow and length-fast calcit and calcitized aragonite in a Holocene speleothem, Carslbad caverns, New Mexico. Journal of Sedimentary Petrology 46, 3, 486-496.

Fontugne, M., Shao, Q., Frank, N., Thil, F., Guidon, N., Boeda, E. 2013. Cross-dating (Th/U-14C) of calcite covering prehistoric paintings at Serra da Capivara National Park, Piaui, Brazil. Radiocarbon 55(2–3):1191–8.

Gázquez, F., Calaforra, J.M., Rull, F., Forti, P., García-Casco, A. 2012. Organic matter of fossil origin in the amberine speleothems from El Soplao Cave (Cantabria, Northern Spain). International Journal of Speleology, 41(1), 12.

Genty, D., Baker A., Massault, M., Proctor, C., Pons-Branchu, E., Hamelin, B. 2001. Dead carbon in stalagmites : carbonates bedrocks vs ageing of soil organic matter. Implications for ^{13}C variations in speleothems. Geochim. et Cosmochim. Acta, 65 (20) : 3443-3457

Hellstrom, J., 2006. U–Th dating of speleothems with high initial 230Th using stratigraphical constraint: Quaternary Geochronology, v. 1, p.289–295.

Hoffmann, D.L., Standish, C.D., García-Diez, M., Pettitt, P.B., Milton, J.A., Zilhão, J., Alcolea-González J.J., Cantalejo-Duarte P., Colado H, de Balbin Lorblanchet, M., Ramos-Muños J., Weniger G-Ch, Pike A.W.G. 2018. U-Th dating of carbonate crusts reveals Neandertal origin of Iberian cave art. Science, 359(6378), 912-915.

Hoffmann, D.L., Standish, C.D., Garcia-Diez, M., Pettitt, P.B., Milton, J.A., Zilhao, J., Alcolea-Gonzalez, J.J., Cantalejo-Duarte, P., Collado, H., De Balbín, R. and Lorblanchet, M., 2019. Response to Aubert et al.'s reply 'Early dates for "Neanderthal cave art" may be wrong'[J. Hum. Evol. 125 (2018), 215-217]. J Hum Evol, 135(102644), pp.10-1016.

Hoffmann, D.L., Standish, C.D., García-Diez, M., Pettitt, P.B., Milton, J.A., Zilhão, J., Alcolea-González, J.J., Cantalejo-Duarte, P., Collado, H., de Balbín, R. and Lorblanchet, M., 2020. Response to White et al.'s reply:'Still no archaeological evidence that Neanderthals created Iberian cave art'[J. Hum. Evol.(2020) 102640]. J. Hum. Evol, 144, p.102810.

Huang, C. K., Kerr, P. F. 1960. Infrared study of the carbonate minerals. American Mineralogist: Journal of Earth and Planetary Materials, *45*(3-4), 311-324.

Jiménez de Cisneros, C.J., Caballero, E., Vera, J.A., Durán, J. J., Juliá, R. 2003. A record of Pleistocene climate from a stalactite, Nerja Cave, southern Spain. Palaeogeography, Palaeoclimatology, Palaeoecology, 189(1-2), 1-10.

Jiménez de Cisneros, C. J., Caballero, E. 2011. Carbon isotope values as paleoclimatic indicators. Study on stalagmite from Nerja Cave, South Spain. Carbonates and Evaporites, 26(1), 41-46.

Kocbach, A., Li, Y., Yttri, K.E., Cassee, F.R., Schwarze, P.E., Namork, E. 2006. Physicochemical characterisation of combustion particles from vehicle exhaust and residential wood smoke. Particle and Fibre Toxicology, 3:1.

Lachniet, M.S., Bernal, J.P., Asmerom, Y., Polyak, V. 2012. Uranium loss and aragonite–calcite age discordance in a calcitized aragonite stalagmite. Quat. Geochro., 14, 26-37.

Lindauer, S., Milano, S., Steinhof, A., Hinderer, M. 2018. Heating mollusc shells-A radiocarbon and microstructure perspective from archaeological shells recovered from Kalba, Sharjah Emirate, UAE. Journal of Archaeological Science: Reports, 21, 528-537.

Martínez-Pillado, V., Aranburu, A., Yusta, I., Stoll, H., Arsuaga, J.L. 2010. Clima y ocupaciones en la Galería de Estatuas (Atapuerca, Burgos) en los últimos 14.000 años: Relatos de una estalagmita. MUNIBE (Antropologia-Arkeologia), 61, 89-102.

Martín-García, R., Alonso-Zarza, A.M., Frisia, S., Rodríguez-Berriguete, Á., Drysdale, R., Hellstrom, J. 2019. Effect of aragonite to calcite transformation on the geochemistry and dating accuracy of speleothems. An example from Castañar Cave, Spain. Sedimentary Geology, 383, 41-54.

Martín-García, R., Alonso-Zarza, A. M., Martín-Pérez, A. 2009. Loss of primary texture and geochemical signatures in speleothems due to diagenesis: evidences from Castañar Cave, Spain. Sedimentary geology, 221(1-4), 141-149.

Martín-García, R., Alonso-Zarza, A.M., Martín-Pérez, A., Schröder-Ritzrau, A., Ludwig, T., 2014. Relationships between colour and diagenesis in the aragonite-calcite speleothems in Basajaún Etxea cave, Spain. Sedimentary Geology 312, 63–75.

Medina Alcaide M.A. 2019. Iluminando la oscuridad de las cuevas con manifestaciones gráficas paleolíticas: una visión integral e interdisciplinar del Contexto Arqueológico Interno y de los carbones de madera/ Lighting the darkness of the caves with Paleolithic Art: an integral and interdisciplinary vision of the Internal Archaeological Context and the wood charcoals. Tesis doctoral Inédita. Universidad del País Vasco (UPV/EHU). Vitoria-Gasteiz

Medina-Alcaide, M.A., Torti, J.L. S., Zapata Peña, L. 2015. Lighting the dark: Wood charcoal analysis from Cueva de Nerja (Málaga, Spain) as a tool to explore the context of Palaeolithic rock art. Comptes Rendus Palevol 14 (5): 411-422.

Medina-Alcaide M.A, Sanchidrián J.L. 2014. Hacia el lado oscuro: cueva de Nerja a la luz de los nuevos datos. In Cien años de arte rupestre paleolítico (pp. 133-141). Ediciones Universidad de Salamanca.

McMillan, E.A., Fairchild, I.J., Frisia, S., Borsato, A., McDermott F. 2005. Annual trace element cycles in calcite–aragonite speleothems: evidence of drought in the western Mediterranean 1200–1100 yr BP. Journal of Quaternary Science. 20(5), 423-433.

Mook WG., Van Der Plicht J. 1999. Reporting 14C activities and concentrations. Radiocarbon, 41(3), 227-239

Moreau, C., Messager, C., Berthier, B., Hain S., Thellier, B., Dumoulin, J.P., Caffy, I., Sieudat, M., Beck, L., 2020. ARTEMIS, The 14C AMS facility of the LMC14 National Laboratory: a status report on quality control and microsample procedures. Radiocarbon 62, 1755-1770.

Ortega, R., Maire, R., Devès, G., Quinif, Y. 2005. High-resolution mapping of uranium and other trace elements in recrystallized aragonite–calcite speleothems from caves in the Pyrenees (France): implication for U-series dating. Earth and Planet. Sci. Letters, 237(3-4), 911-923.

Pawlyta, M., Hercman, H. 2016. Transmission electron microscopy (TEM) as a tool for identification of combustion products: Application to black layers in speleothems. In Annales Societatis Geologorum Poloniae 86, 237–248.

Pearce, D. G., Bonneau, A. 2018. Trouble on the dating scene. Nature ecology & evolution, 2(6), 925-926.

Perrin, C., Prestimonaco, L., Servelle, G., Tilhac, R., Maury, M., Cabrol, P. 2014. Aragonite–calcite speleothems: identifying original and diagenetic features. Journal of Sedimentary Research, 84(4), 245-269.

Pike, A.W.G., Hoffmann, D.L., García-Diez M., Pettitt P.B., Alcolea J., De Balbín, R., González-Sainz, C, de las Heras, C, Lasheras, J.A., Montes, R, Zilhão J. 2012. U-series dating of Paleolithic Art in 11 Caves in Spain. Science 336:1409–13.

Pons-Branchu, E., Hillaire-Marcel, C., Ghaleb, B., Deschamps, P., Sinclair, D. 2005. Early diagenesis impact on precise U-series dating of Deep-Sea corals. Example of a 100-200 years old Lophelia Pertusa sample from NE Atlantic. Geochim. et Cosmochim. Acta, 69(20) :4865-4879.

Pons-Branchu, E., Bourrillon, R., Conkey, M., Fontugne, M., Fritz, C., Gárate, D., Quiles, A., Rivero, O, Sauvet, G., Tosello, G., Valladas, H., White, R. 2014a. U-series dating of carbonate formations overlying Paleolithic art: interest and limitations. Bulletin de la Société préhistorique française, Tome 111, numéro 2, avril-juin 2014, p. 211-224

Pons-Branchu, E., Douville, E., Roy-Barman, M., Dumont, E., Branchu, P., Thil, F., Frank, N., Bordier, L., Borst. W. 2014b. A geochemical perspective on Parisian urban history based on U-Th dating, laminae counting and yttrium and REE concentrations of recent carbonates in underground aqueducts. Quaternary Geochronology 24, 44-53.

Pons-Branchu, E., Sanchidrian, J.L., Fontugne, M., Medina Alcaide, M.A., Quiles, A., Thil, F., Valladas, H. 2020. U-series dating at Nerja cave reveal open system. Questioning the Neanderthal origin of Spanish rock art. Journal of Archaeological Science. 117 – 105120.

Pulido-Bosch, A., Martin-Rosales, W., López-Chicano, M., Rodriguez-Navarro, C. M., Vallejos, A. 1997. Human impact in a tourist karstic cave (Aracena, Spain). Environmental geology, 31(3), 142-149

Railsback, L.B., Dabous, A.A., Osmond, J.K., Fleisher, C.J. 2002. Petrographic and geochemical screening of speleothems for U-series dating: an example from recrystallized speleothems from Wadi Sannur Cavern, Egypt. J. of Cave and Karst Studies, 64(2), 108-116.

Railsback, L.B., Brook, G.A., Chen, J., Kalin, R., Fleisher, C.F. 1994. Environmental controls on the petrology of a late Holocene speleothem from Botswana with annual layers of aragonite and calcite. Journal of sedimentary research A64 (1), 147-155.

Railsback, L.B., Liang, F., Romaní, J.R.V., Grandal-d'Anglade, A., Rodríguez, M.V., Fidalgo, L.S., Fernandez Mosquera D., Cheng H., Edwards, R.L. 2011. Petrographic and isotopic evidence for Holocene long-term climate change and shorter-term environmental shifts from a stalagmite from the Serra do Courel of northwestern Spain, and implications for climatic history across Europe and the Mediterranean. Palaeogeography, Palaeoclimatology, Palaeoecology, 305(1-4), 172-184.

Ramsey, C. B. 2006. New approaches to constructing age models: OxCal4. Radiocarbon, 400, 500.

Reimer, P.J., Austin, W.E.N., Bard, E., Bayliss, A., Blackwell, P.G., Ramsey, C.B., Butzin, M., Cheng, H., Edwards, R.L., Friedrich, M., Grootes, P.M., Guilderson, T.P., Hajdas, I., Heaton, T.J., Hogg, A.G., Hughen, K.A., Kromer, B., Manning, S.W., Muscheler, R., Palmer, J.G., Pearson, C., van der Plicht, J., Reimer, R.W., Richards, D.A., Scott, E.M., Southon, J.R., Turney, C.S.M., Wacker, L., Adophi, F., Büntgen, U., Capano, M., Fahrni, S., Fogtmann-Schulz, A., Friedrich, R., Köhler, P., Kudsk, S., Miyake, F., Olsen, J., Reinig, F., Sakamoto, M., Sookdeo, A., Talamo, S., 2020. The IntCal20 Northern Hemisphere radiocarbon calibration curve (0-55 kcal BP). Radiocarbon 62, 725-757.

Rossi, C., Lozano, R.P. 2016. Hydrochemical controls on aragonite versus calcite precipitation in cave dripwaters. Geochimica et Cosmochimica Acta, 192, 70-96.

Sánchez-Moral, S., Soler, V., Cañaveras, J.C., Sanz-Rubio, E., Van Grieken, R., Gysels, K. 1999. Inorganic deterioration affecting the Altamira Cave, N Spain: quantitative approach to wall-corrosion (solutional etching) processes induced by visitors. Science of the total environment, 243, 67-84.

Sanchidrián, J., Márquez, A.M., Valladas, H, Tisnerat, N. 2001. Dates directes pour l'art rupestre d'Andalousie (Espagne). International Newsletter on Rock Art 29:15–19.

Sanchidrián, J.L., 1994. Arte Rupestre de la Cueva de Nerja. Fundación Cueva de Nerja, Málaga

Sanchidrián, J.L., Valladas, H., Medina Alcaide, M.A.., Pons-Branchu, E., Quiles, A. 2017. New perspectives for 14C dating of parietal markings using CaCO$_3$ thin layers: an example in Nerja cave (Spain). Journal of Archaeological Science reports 12. pp 74-80.

Sanz de Galdeano, C. 1990. Estructura y estratigrafía de la Sierra de los Guájares y sectores próximos (conjunto Alpujárride, Cordilleras Béticas). Estudios geológicos, 46(1-2), 123-134.

Scholz, D., Tolzmann, J., Hoffmann, D. L., Jochum, K. P., Spötl, C., Riechelmann, D. F. 2014. Diagenesis of speleothems and its effect on the accuracy of 230Th/U-ages. Chemical Geology, 387, 74-86.

Shao, Q.F., Pons-Branchu, E., Zhu, Q.P., Wei Wang, W., Valladas, H., Fontugne, M. 2017. High precision U/Th dating of the rock paintings at Mt. Huashan, Guangxi, southern China. Quaternary research, 88 (1) 1-13.

Shao, Q.F., Wu, Y., Pons-Branchu, E., Zhu, Q., Dapoigny, A., Jiang T. 2021. U-series dating of the rock paintings in Cangyuan, southwestern China. In review à Quaternary Geochronology. Quaternary Geochronology. 61 - 101127

Slimak, L., Fietzke, J., Geneste, J.M., Ontañón, R. 2018. Comment on "U-Th dating of carbonate crusts reveals Neandertal origin of Iberian cave art". Science, 361(6408), eaau1371.

Tisnérat–laborde, N., Poupeau, J.J., Tannau, J.F., Paterne, M. 2001. Development of a Semi-Automated System for Routine Preparation of Carbonate Samples. Radiocarbon, 2001, 43 (2A), pp.299-304.

Toffolo, M.B. 2021. The significance of aragonite in the interpretation of the microscopic archaeological record. Geoarchaeology, 36(1), 149-169.

Thompson, W. G., Spiegelman, M. W., Goldstein, S. L., Speed, R. C. (2003). An open-system model for U-series age determinations of fossil corals. Earth and Planetary Science Letters, *210*(1-2), 365-381.

Valladas, H., Pons-Branchu, E., Dumoulin, J.P., Quiles, A., Medina-Alcaide, M.A., Sanchidrian JL. 2017. U/Th and C-14 cross dating of parietal calcite deposits: application to Nerja cave (Andalusia, Spain) and future perspectives. Radiocarbon 59 (6). 1955-1967

Wassenburg, J.A., Immenhauser, A., Richter, D.K., Jochum, K.P., Fietzke, J., Deininger, M., Goos, M., Scholz, D., Sabaoui, A. 2012. Climate and cave control on Pleistocene /Holocene calcite-to-aragonite transitions in speleothems from Morocco: elemental and isotopic evidence. Geochimica et Cosmochimica Acta, 92, 23-47.

White, R., Bosinski, G., Bourrillon, R., Clottes, J., Conkey, M.W., Rodriguez, S.C., et al. 2020. Still no archaeological evidence that Neanderthals created Iberian cave art. J. Hum. Evol, 144, 102640.

Wu, Y., Jiao, Y., Ji, X., Taçon, P.S.C., Yang, Z., He, S., Jin, M., Li, Y., Shao, Q. 2022. High-precision U-series dating of the late Pleistocene – early Holocene rock paintings at Tiger Leaping Gorge, Jinsha River valley, southwestern China. Journal of Archaeological Science 138. 105535.

Zhang, H., Cai, Y., Tan, L., Qin, S., An, Z. 2014. Stable isotope composition alteration produced by the aragonite-to-calcite transformation in speleothems and implications for paleoclimate reconstructions. Sedimentary Geology, 309, 1-14.
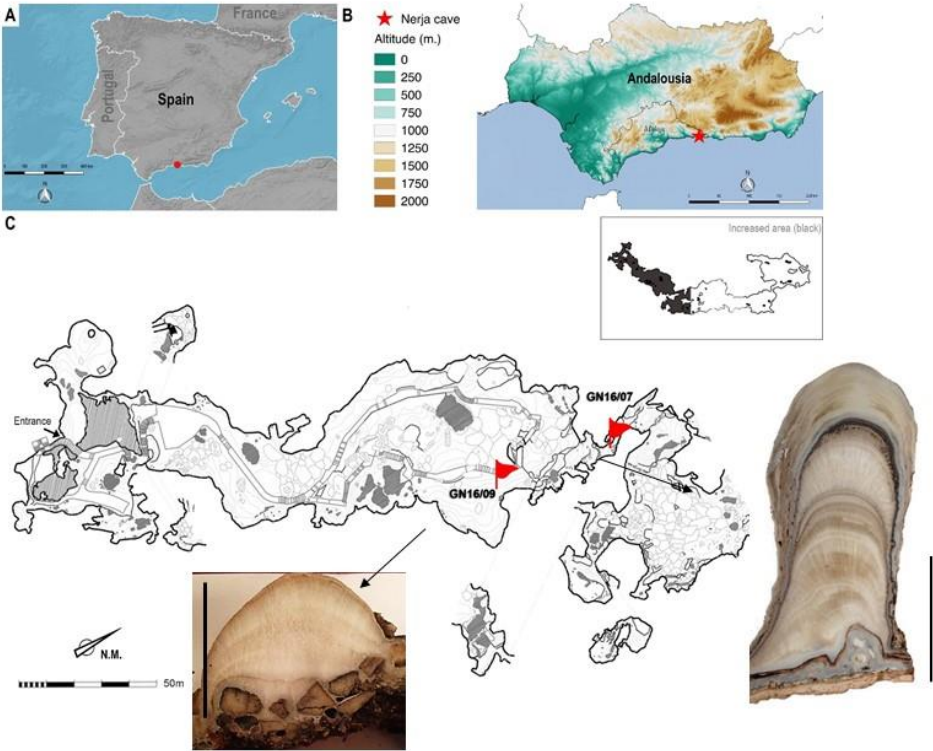
Figure caption

Figure 1: Location of Nerja cave, in Southern Spain (A and B), and map of the cave with sample location and pictures (C). Vertical bar is 5 cm.
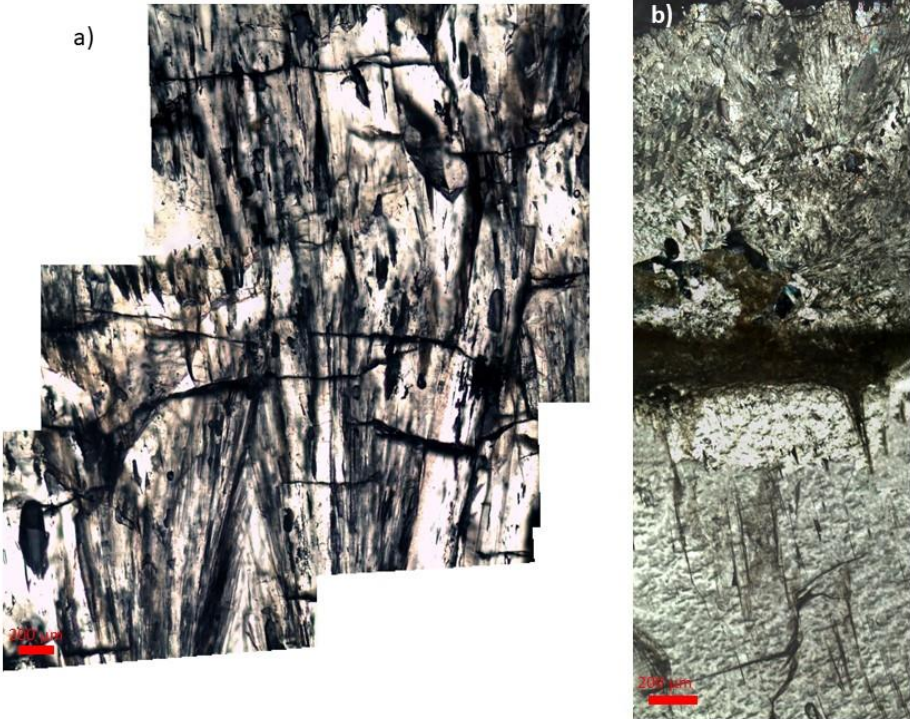
Figure 2: Petrographic study of stalagmite GN 16-9b: a) aragonite fibers in plane polarized light; b) cross-polarized image of the outer layer. Red horizontal bar is 200 μm.
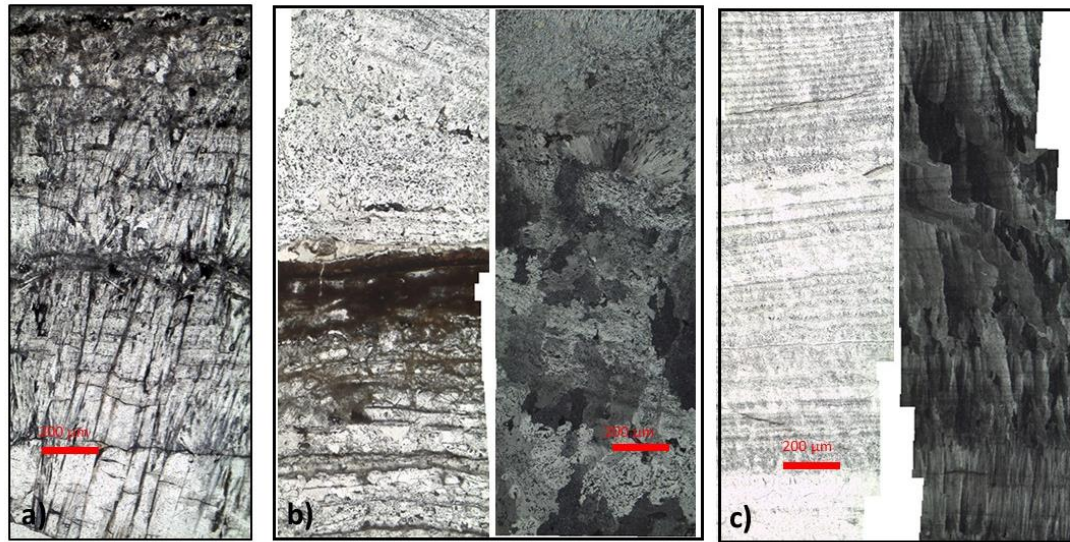

Figure 3 Petrographical observations of GN16-7 stalagmite a) : aragonite fibers in the central part of the speleothem observed in plane polarized light; b) the bottom part of the sample is marked by alternating light and dark levels that are formed by mosaic crystals ; the transition with the intermediate part is underlined by the presence of fan-shaped fibers; c) finely laminated material is observed on the top of the sample using plane polarized light but acicular fibers are revealed by cross polar light. Horizontal bar is 200 μm.

Figure 4: GN16-7 stalagmite: the mineralogy was determined by FTIR using the wavenumber of the v2 band. ^{230}Th/^{234}U and ^{14}C ages are compared for the different analytical points (red dots). The areas where age differences between the two dating methods exist correspond to a change in mineralogy and notably the presence of calcite.
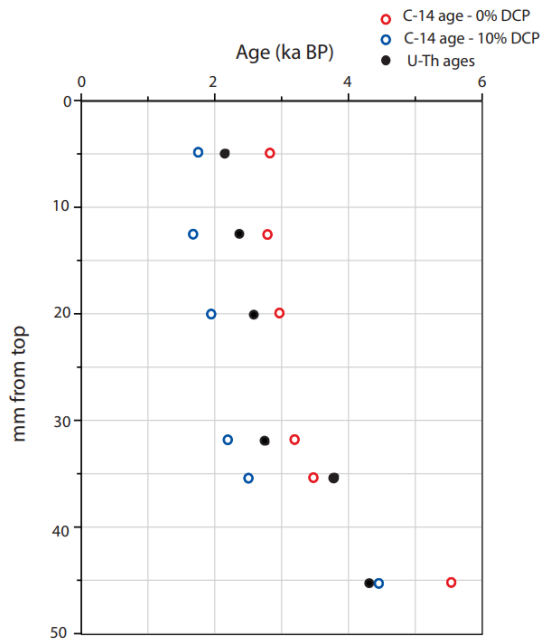
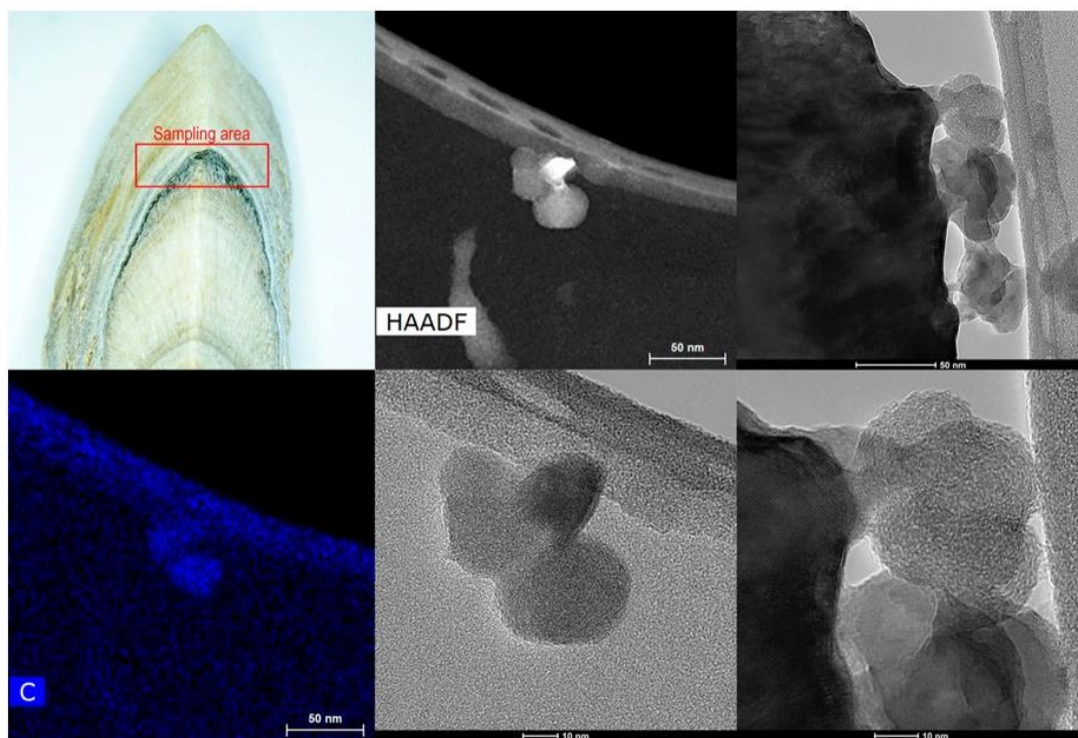Figure 5: ^{230}Th/^{234}U and ^{14}C ages for stalagmite GN 17-9b

Figure 6: Detail of the black level analyzed in sample GN16-7 and pictures of the soot aggregate nanoparticles and their Carbon composition (image bottom left).
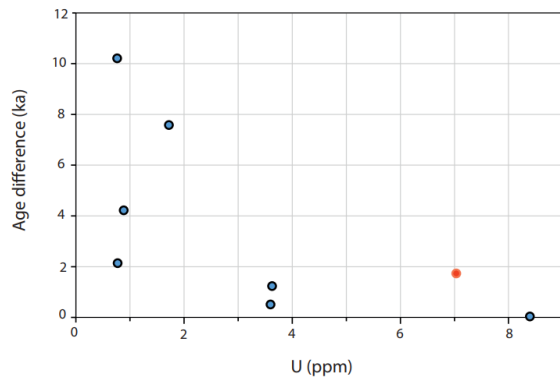
Figure 7: Age difference (^{230}Th/^{234}U - ^{14}C ages) for stalagmite GN 16-7. Red dot is the sample taken at 105 mm from top. ^{14}C was not determined for this sample, and real age is assumed according to sampling position by a linear extrapolation between samples before and after.

Figure 8: Picture of the dark soot layers of stalagmite GN 16-7
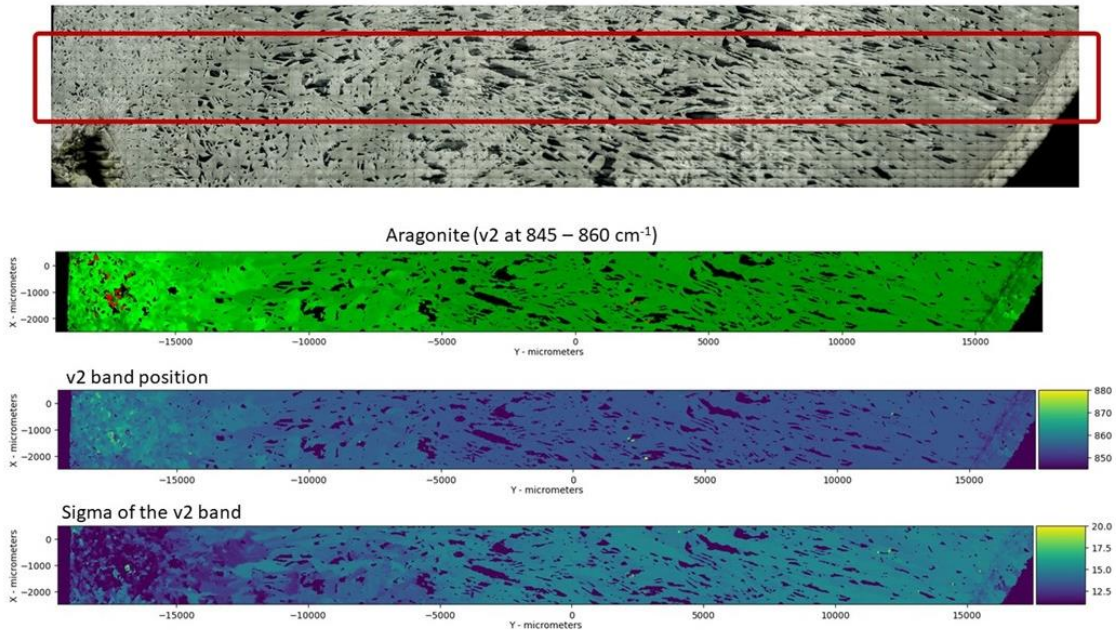
Supplementary material

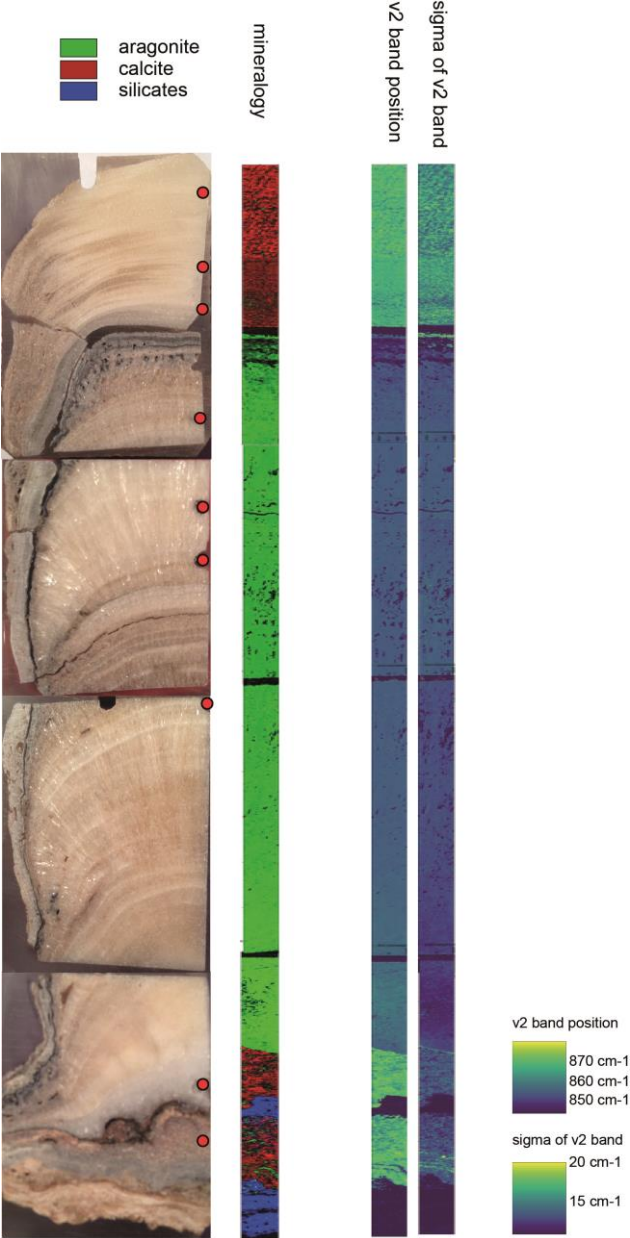Figure S.M. 1: Mineralogy of the GN16-9b stalagmite determined by FTIR using the wavenumber of the v2 band.

.

Figure S.M.2: Mineralogy of the GN16-7 stalagmite determined by FTIR using the wavenumber of the v2 band